Suitably impressive thesis title

Mikkel Bjørn
St. Anne's College
University of Oxford

A thesis submitted for the degree of
Doctor of Philosophy
Trinity 2020

Acknowledgements

suitable thank you's

Abstract

World's best measurement of γ. Details to be added.

Contents

Preface

The work presented in this thesis has been resulted in two papers, either under review or published in the Journal of High Energy Physics. These are

[1] *Measurement of the CKM angle γ using $B^\pm \to [K^0_S h^+ h^-]_D h^\pm$ decays*, submitted to JHEP.
This paper describes a measurement of the CKM angle γ using pp collision data taken with the LHCb experiment during the Run 1 of the LHC, in 2011 and 2012, and during the full Run 2, in 2015–2018. The measurement uses the decay channels $B^\pm \to Dh^\pm$ where $D \to K^0_S h'^+ h'^-$, in which h and h' denotes pions or kaons. It obtains a value of $\gamma = (?\pm?)^\circ$, which constitutes the world's best single-measurement determination of γ. The work is the main focus of this thesis and described in detail in Chapter 5.

[2] *CP violation and material interaction of neutral kaons in measurements of the CKM angle γ using $B^\pm \to DK^\pm$ decays where $D \to K^0_S \pi^+ \pi^-$*, JHEP 19 (2020) 106.
This paper describes a phenomenological study of the impact of neutral kaon CP violation and material interaction on measurements of γ. With the increased measurement precision to come in the near future, an understanding of these effects is crucial, especially in the context of $B \to D\pi$ decays; however no detailed study had been published at the start of this thesis. The study is the subject of Chapter 4.

All of the work described in this thesis is my own, except where clearly referenced to others. Furthermore, I contributed significantly to an analysis of $B^\pm \to DK^\pm$ decays with LHCb data taken in 2015 and 2016, now published in

[3] *Measurement of the CKM angle γ using $B^\pm \to DK^\pm$ with $D \to K^0_S \pi^+ \pi^-$ $K^0_S K^+ K^-$ decays*, JHEP 08 (2018) 176.

I was responsible for the analysis of the signal channel, whereas the control channel was analysed by Nathan Jurik. The measurement is superseded by that of Ref. [1] and is not described in detail in the thesis.

1 Introduction

All the big picture stuff: constraints on New Physics from high precision measurements, a small nod to matter-antimatter asymmetry questions etc.

1.1 Structure of the thesis

2

Theoretical background

This chapter lays out the theoretical framework of the thesis. Section 2.1 introduces charge and parity symmetry violation in general, while Section 2.2 covers the description in the Standard Model and the general theory behind charge-parity symmetry violation measurements in charged B decays. Section 2.3 focuses on the theory of measurements using $B^{\pm} \to Dh^{\pm}$ decays with multi-body D final states, after which the specific analysis strategy for the measurement described in the thesis is outlined out in Section 2.4.

2.1 The C, P and T symmetries and their violation

The concept of symmetry play a fundamental role in modern physics. By Noether's theorem [4], the simple assumption of invariance of our physical laws under universal temporal and spatial translations leads to the very non-trivial prediction of conserved energy and momentum; within the field of particle physics, the interactions and dynamics of Standard Model (SM) follow completely simply from requiring the fundamental particle fields to satisfy a local $U(1) \times SU(2) \times SU(3)$ gauge symmetry [5]; and one of the short-comings of the SM, is that it fails to explain the apparent *lack* of symmetry in our matter-dominated universe [6]. Indeed, it is important to experimentally establish the symmetries of our world at a fundamental level, and the degree to which they are broken.

I'll adjust this paragraph when I've written the introduction.

Three discrete symmetries of importance are the symmetries under

1. The charge operator C, which conjugates all internal quantum numbers of a quantum state and thus converts particles into their anti-particle counter parts. For example, C transforms the electric charge of a particle state $Q \to -Q$.

2. The parity operator P, which inverts the spatial dimensions of space time: $\vec{x} \to -\vec{x}$. As such, it transforms left-handed particle fields into right-handed particle fields and vice versa.

3. The time-inversion operator T, which inverts the temporal dimension of space time: $t \to -t$.

These are fundamentally related by the CPT theorem [7] , which states that any Lorentz-invariant Quantum Field Theory (QFT) must be symmetric under the simultaneous application of *all* three operators. However, any one of the symmetries can be broken individually, and experiments have shown the physical laws of our world to violate each of the C, P, and T symmetries.

Such a symmetry-breaking effect was established for the first time in 1956, when Chien-Shiung Wu observed parity violation in weak decays of Co-60 nuclei [8], after carrying out an experiment that was proposed by Yang Chen-Ning and Tsung-Dao Lee [9]. While this experiment established the breaking of P symmetry, it left open the possibility that the physical laws are invariant under a combination of a charge- and parity inversion; that they are CP symmetric. However, this was disproved in 1964 when Kronin and Fitch observed that long-lived kaons, which predominantly decay to the CP-odd 3π state, could also decay to the CP-even $\pi\pi$ states [10].

Since then CP violation has been found in the B^0 system by the BaBar and Belle collaborations [11,12] during the early 2000's; the B factories, along with CDF, also saw evidence for CP violation in $B^\pm$ decays [13–18] later confirmed by LHCb [19], and CP violation was measured for the B_s^0 meson by LHCb in 2013 [20]; within the last year and a half, the first observation of CP-violation in D^0 decays has also been made by the LHCb collaboration [21], and most recently evidence for CP-violation in the neutrino sector has been reported by the T2K collaboration [22]. The observed effects can be divided into distinct classes. The conceptually simplest case is

1. *CP-violation in decay*, where $|A/\bar{A}| \neq 1$ for some decay amplitude A, and the amplitude $\bar{A}$ of the CP-conjugate decay. The result is different decay rates in two CP-conjugate decays

$$\Gamma(M \to f) \neq \Gamma(\bar{M} \to \bar{f}). \tag{2.1}$$

This type of *CP* violation was not seen until the late 1980ies [23, 24], more than 20 years after the first observation of *CP* violation, and only finally established around the year 2000 [25, 26]. Also this discovery was made in $K \to \pi\pi$ decays.

CP-violation in decay is the only type possible for charged initial states, and it is thus the main focus of the thesis. Two additional *CP*-violating effect are possible for neutral initial states (a situation that will be the main focus of Chapter 4). These effects are

2. *CP-violation in mixing*, which denotes the case where the mixing rates between the M^0 and $\bar{M}^0$ states differ

$$\Gamma(M^0 \to \bar{M}^0) \neq \Gamma(\bar{M}^0 \to M^0). \tag{2.2}$$

The *CP* violation first observed by Kronin and Fitch in the neutral kaon sector [10] is (dominantly) of this type.

3. *CP-violation in interference between mixing and decay*, which can be present for a neutral initial states M^0 decaying into a final state f common to both M^0 and $\bar{M}^0$. The decay rate includes an interference term between two amplitudes: the amplitude for a direct $M^0 \to f$ decay and the amplitude for a decay after mixing: $M^0 \to \bar{M}^0 \to f$. Even in the absence of the two aforementioned effects, the rates $\Gamma(M^0 \to f)$ and $\Gamma(\bar{M}^0 \to \bar{f})$ can differ due to the interference term. Such *CP* asymmetries have been measured in eg. $B^0 \to J/\psi K$ by LHCb and the B factories, and in $B_s^0 \to J/\psi\phi$ decays by the LHC and Tevatron experiments [27].

CP violation measurements thus have a long, rich, and still-developing history.

2.2 CP violation in the Standard Model

All existing measurements of *CP* violation in the quark sector are naturally explained in the SM; indeed, the need to explain the observation *CP* violation in neutral kaons was a driving force in the development of the model in the first place, when it lead Kobayashi and Maskawa to predict the existence of then-unknown particles in 1973 [28] (now known to be the third generation quarks).

2.2.1 The CKM matrix and the Unitarity Triangle

The SM contains three generations of quarks, each consisting of an up-type quark (u, c, and t) and a down-type quark (d, s, and b). The charged weak interaction of the $W^{\pm}$ boson couples up and down-type quarks. The quark states that couple to the W are not (a priori) identical to the mass eigenstates, and can be denoted (u', c', and t') and (d', s', and b'). A basis for the quark states can be chosen such that the weakly coupling up-quark states are identical to the propagating quark states, $u = u'$, but then the down-type quark stare are different: $d' \neq d$. The two bases of the down-type quarks are related via the Cabibbo-Kobayashi-Maskawa (CKM) matrix [28, 29][1]

$$\begin{pmatrix} d' \\ s' \\ t' \end{pmatrix} = V \begin{pmatrix} d \\ s \\ t \end{pmatrix} = \begin{pmatrix} V_{ud} & V_{us} & V_{ub} \\ V_{cd} & V_{cs} & V_{cb} \\ V_{td} & V_{ts} & V_{tb} \end{pmatrix} \begin{pmatrix} d \\ s \\ t \end{pmatrix}. \tag{2.3}$$

Thus the Lagrangian terms representing the coupling of a $W^{\pm}$ boson with a u- and a d-type quark is

$$\mathcal{L}_{W^+} = -\frac{g}{\sqrt{2}} V_{ud} \left(\bar{u} \gamma^{\mu} W_{\mu}^{+} d \right) \qquad \mathcal{L}_{W^-} = -\frac{g}{\sqrt{2}} V_{ud}^{*} \left(\bar{d} \gamma^{\mu} W_{\mu}^{-} u \right) \tag{2.4}$$

where g is the weak coupling constant, γ_u are the Dirac matrices, and u and d represent the left-handed components of the physical quark states.

The CKM matrix is a unitary complex 3×3 matrix, and hence has $3^2 = 9$ independent, real parameters. However, 5 of these can be absorbed into non-physical phases of the quark states (both mass and weak eigenstates) and hence the matrix has 4 real, physical parameters: 3 mixing angles and a single phase. Chau and Keung [30] proposed the parameterisation

$$\begin{aligned} V &= \begin{pmatrix} 1 & 0 & 0 \\ 0 & c_{23} & s_{23} \\ 0 & -s_{23} & c_{23} \end{pmatrix} \begin{pmatrix} c_{13} & 0 & s_{13} e^{-i\delta_{CP}} \\ 0 & 1 & 0 \\ -s_{13} e^{-i\delta_{CP}} & 0 & c_{13} \end{pmatrix} \begin{pmatrix} c_{12} & s_{12} & 0 \\ -s_{12} & c_{12} & 1 \\ 0 & 0 & 1 \end{pmatrix} \\ &= \begin{pmatrix} c_{12} c_{13} & s_{12} c_{13} & s_{13} e^{-i\delta_{CP}} \\ -s_{12} c_{23} - c_{12} s_{23} s_{13} e^{i\delta_{CP}} & c_{12} c_{23} - s_{12} s_{23} s_{13} e^{i\delta_{CP}} & s_{23} c_{13} \\ s_{12} s_{23} - c_{12} c_{23} s_{13} e^{i\delta_{CP}} & -c_{12} s_{23} - s_{12} c_{23} s_{13} e^{i\delta_{CP}} & c_{23} c_{13} \end{pmatrix} \end{aligned} \tag{2.5}$$

which is the preferred standard by the PDG [31]. Here, $s_{ij} \equiv \sin\theta_{ij}$ and $c_{ij} \equiv \cos\theta_{ij}$ denote the sine and cosine of three rotation angles in quark space; $\theta_{12} = \theta_C$ being the usual Cabibbo angle [29].

[1] A basis for the quarks can of course be chosen, such that neither the up-quarks or the down-quarks are expressed in their mass eigenstates. In that case the CKM matrix is recovered as $V = U_u^* U_d$, where $U_{u/d}$ is the unitary transformation matrices that brings the u/d quarks into their mass eigenstates.

The presence of the complex phase δ_{CP} in the Lagrangian term of the W coupling causes *CP* violation because, as evident from Eq. (2.4), if δ_{CP} enters the amplitude for some decay mediated by a W boson, $A = |A|e^{i(\delta_0+\delta_{CP})}$, then it will enter the *CP* conjugate decay amplitude with the opposite sign: $\bar{A} = |A|e^{i(\delta_0-\delta_{CP})}$. In these expressions, δ_0 denotes a *CP* conserving phase that is not caused by complex terms in the Lagrangian, but arises due to potential intermediate states in the decay amplitude.[2] Usually the underlying mechanism is due to QCD effects, and these *CP* conserving phases are therefore generally dubbed *strong* phases, as opposed to the *CP* violating *weak* phase of the W coupling [31]. This terminology will be applied throughout the thesis.

Experimentally, it has been observed that the CKM matrix elements of Eq. (2.5) satisfy $s_{13} \ll s_{23} \ll s_{12}$. This motivates an often used, alternative parameterisation of the matrix, where the elements are expressed as power series in a parameter λ that naturally incorporates this hierarchy: the Wolfenstein parameterisation [32]. The definitions

$$\begin{aligned} s_{12} &\equiv \lambda \\ s_{23} &\equiv \lambda^2 A \\ s_{13} &\equiv \lambda^3(\rho - i\eta) \end{aligned} \tag{2.6}$$

are made, after which the unitarity conditions (or Eq. 2.5) determine the remaining elements to any order in λ.[3] To $\mathcal{O}(\lambda^5)$ the Wolfenstein parameterisation of the CKM matrix is [34, 35]

$$V = \begin{pmatrix} 1 - \frac{\lambda^2}{2} - \frac{\lambda^4}{8} & \lambda & A\lambda^3(\rho - i\eta) \\ -\lambda + \frac{\lambda^5}{2}A^2(1 - 2(\rho + i\eta)) & 1 - \frac{\lambda^2}{2} - \frac{\lambda^4}{8}(1 + 4A^2) & A\lambda^2 \\ A\lambda^3(1 - (\rho + i\eta)(1 - \frac{\lambda^2}{2})) & -A\lambda^2(1 - \frac{\lambda^2}{2}(1 - 2(\rho + i\eta))) & 1 - \frac{1}{2}A^2\lambda^4 \end{pmatrix}. \tag{2.7}$$

The unitarity condition $V^\dagger V = \mathbb{1}$ of the CKM matrix defines 9 relations between the CKM elements of the form

$$\sum_j V_{jq}^* V_{jq} = 1 \quad , \quad q \in \{d, s, b\} \qquad \text{along the diagonal} \tag{2.8a}$$

$$\sum_j V_{jq}^* V_{jq'} = 0 \quad , \quad q, q' \in \{d, s, b\}, q \neq q' \qquad \text{off-diagonal.} \tag{2.8b}$$

[2] It is generally true that all phases of a single term in a given amplitude will be convention dependent, but that the phase differences between terms are not.

[3] Other variants of the Wolfenstein parameterisation do exist [33]. They all agree at the lowest orders of λ.

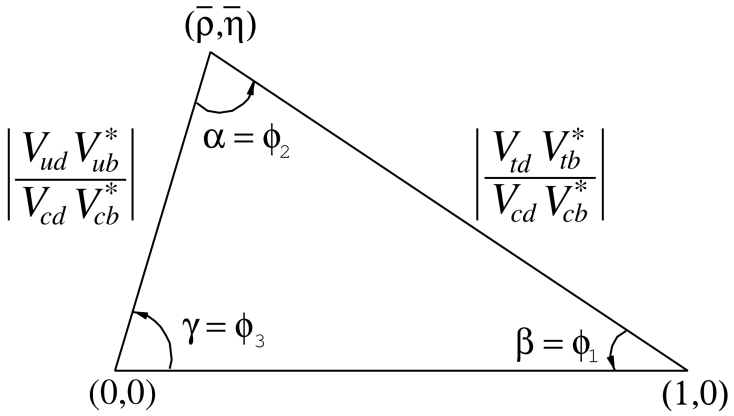

Figure 2.1: Definition of the lengths and sides of the Unitarity Triangle. Figure is taken from the *CKM Quark-Mixing Matrix* review of the PDG [31].

The off-diagonal conditions constrain three complex numbers to sum to zero, and can thus be visualised as triangles in the complex plane, the so-called unitarity triangles. Of these, the triangle corresponding to the (d, b) elements plays a special role, because all three sides are of the same order of magnitude, $\mathcal{O}(\lambda^3)$. When expressed in the form

$$\frac{V_{ud}^* V_{ub}}{V_{cd}^* V_{cb}} + \frac{V_{td}^* V_{tb}}{V_{cd}^* V_{cb}} + 1 = 0, \tag{2.9}$$

it is often referred to as the singular Unitarity Triangle, illustrated in Fig. 2.1 where the usual names for the three angles are also given.

Over-constraining the unitarity triangle by making separate measurements of all sides and angles, in as many different decay channels as possible, is an important, and non-trivial test of the SM. The current experimental constraints are in agreement with the SM predictions, as visualised in Fig. 2.2. The CKM angle

$$\gamma \equiv \arg(-V_{ud}V_{ub}^*/V_{cd}V_{cb}^*) = \arg(-V_{cb}V_{cd}^*/V_{ub}V_{ud}^*) \tag{2.10}$$

is uniqu ong the CKM parameters, in th can be measured in tree-level processes w ut significant theoretical uncertainty from lattice QCD calculations [36]. Because tree-level processes are less likely to be affected by Beyond-Standard-Model (BSM) effects, direct measurements of γ can be considered a SM benchmark, which can be compared to estimates based on measurements of other CKM elements that are measured in loop-level processes, and thus are more likely to be affected by BSM effects [37]. The current, worldwide combination of direct measurements, published by the CKMFitter group, is $\gamma = (72.1^{+5.4}_{-5.7})^\circ$, to be compared with the estimate from loop-level observables of $\gamma = (65.66^{+0.90}_{-2.65})^\circ$ [38]. Other world averages

Not sure if I should spend time explaining the non-gamma measurements entering?

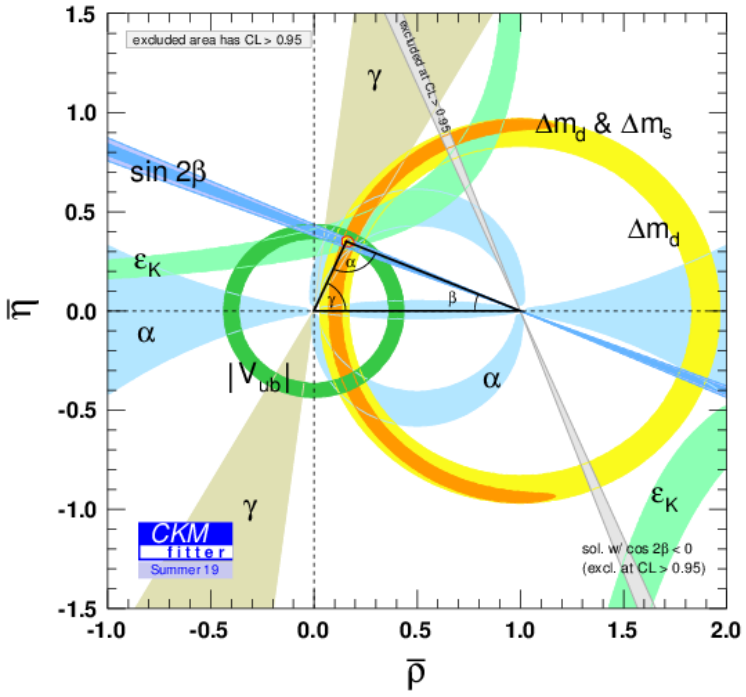

Figure 2.2: Current constraints on the Unitarity Triangle parameters as determined by the CKMFitter group for the EPS 2019 conference [38].

exist [27, 39], but the overall picture is the same: the ability to constrain BSM physics is currently limited by the uncertainty of the direct measurements. Hence further precision measurements of γ are highly motivated. Presently, the precision is driven by time-integrated measurements of direct *CP*-violation in $B^{\pm} \to DK^{\pm}$ decays; such a measurement is the topic of this thesis and the theory behind is treated in detail in the following section. It is also possible to measure γ in time-dependent mixing analyses of $B^0_s \to D^{\mp}_s K^{\pm}$, $B^0 \to D^{\mp}\pi^{\pm}$ and related decays, by measuring *CP* violation in interference between mixing and decay. These modes are expected to provide competitive measurements in the future [40, 41].

2.2.2 Measuring γ in tree level decays

The phase γ can be measured in tree-level processes with interference between $b \to cs\bar{u}$ and $b \to \bar{c}su$ transitions. The canonical example, also the subject of this thesis, is based on measurements sensitive to interference between the $B^{\pm} \to D^0 K^{\pm}$ and $B^{\pm} \to \overline{D}^0 K^{\pm}$ decay amplitudes. As illustrated in Fig. 2.3 for the case of B^- decays, the electro-weak phase difference between the two decays

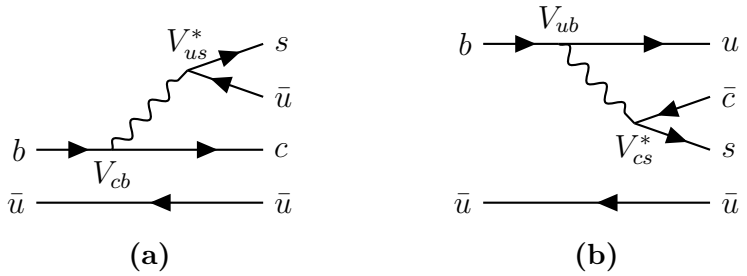

Figure 2.3: Tree level Feynman diagrams describing (a) $B^- \to D^0 K^-$ and (b) $B^- \to \overline{D}^0 K^-$ decays. The electro-weak phase difference between the two decays is $\Delta\phi = \arg\left(V_{cb}V_{us}^*/V_{ub}V_{cs}^*\right) \simeq \gamma$.

is $\Delta\phi = \arg\left(V_{cb}V_{us}^*/V_{ub}V_{cs}^*\right)$. While $\Delta\phi$ is not identical to the definition of γ in Eq. (2.10), the ratio of the involved CKM matrix elements is [42]

$$\begin{aligned} -\frac{V_{cd}^*/V_{ud}^*}{V_{us}^*/V_{cs}^*} &= -\frac{-\lambda[1-\frac{\lambda^4}{2}A^2(1-2(\rho-i\eta))](1-\frac{\lambda^2}{2}-\frac{\lambda^4}{8}(1+4A^2))}{\lambda(1-\frac{\lambda^2}{2}-\frac{\lambda^4}{4})} \\ &= 1-\lambda^4A^2(1-2(\rho-i\eta))+\mathcal{O}(\lambda^5). \end{aligned} \tag{2.11}$$

The ratio equals unity to $\mathcal{O}(\lambda^4) \simeq 2.6 \times 10^{-3}$, and thus $\Delta\phi \simeq \gamma$ is a good approximation within current experimental uncertainties. For the remainder of this thesis the approximation will be used without further comment. The diagrams in Fig. 2.3 describe the leading order contributions to the two amplitudes

$$\begin{aligned} A[B^- \to D^0 K^-] &\equiv A_B \\ A[B^- \to \overline{D}^0 K^-] &\equiv \bar{A}_B \equiv r_B A_B e^{i(\delta_B-\gamma)}, \end{aligned} \tag{2.12a}$$

where the last equality introduces two new parameters: the amplitude magnitude ratio $r_B \equiv |\bar{A}_B|/|A_B|$, and δ_B, the strong-phase difference between the decay amplitudes. Since all *CP*-violation is attributed to the electro-weak phase in the SM, the *CP*-conjugate decay amplitudes are [43]

$$\begin{aligned} A[B^+ \to \overline{D}^0 K^+] &= A_B \\ A[B^+ \to D^0 K^+] &= \bar{A}_B = r_B A_B e^{i(\delta_B+\gamma)}. \end{aligned} \tag{2.12b}$$

In an experimental setting, the D^0 and $\overline{D}^0$ mesons are reconstructed in some final state, f or its *CP*-conjugate $\bar{f}$. In analogy with the $B^\pm$ decays, the D decay amplitude can be related[4]

$$\begin{aligned} A[D^0 \to f] &= A[\overline{D}^0 \to \bar{f}] = A_D \\ A[\overline{D}^0 \to f] &= A[D^0 \to \bar{f}] = r_D A_D e^{i\delta_D}. \end{aligned} \tag{2.13}$$

[4]In this notation δ_D is thus phase of the suppressed D-decay amplitude minus the phase of the favoured D-decay amplitude. This is the opposite convention to that used in the LHCb measurements with the ADS technique, but aligns with the notation used in the literature on γ measurements in $D \to K_S^0\pi^+\pi^-$ decays.

where the assumption has been made that *CP* violation in the D decays is negligible, and δ_D denotes a *CP*-conserving strong-phase difference. While *CP*-violation in D decays has recently been measured [21], the size of the effect is small and it is considered negligible in this thesis. Based on Eqs. 2.12 and (2.13), the decay rates of B^+ and B^- mesons into the possible final states can be seen to satisfy

$$\Gamma(B^- \to D(\to f)K^-) \propto 1 + r_D^2 r_B^2 + 2r_B r_D \cos\left[\delta_B + \delta_D - \gamma\right], \tag{2.14a}$$
$$\Gamma(B^+ \to D(\to \bar{f})K^+) \propto 1 + r_D^2 r_B^2 + 2r_B r_D \cos\left[\delta_B + \delta_D + \gamma\right], \tag{2.14b}$$
$$\Gamma(B^- \to D(\to \bar{f})K^-) \propto r_D^2 + \ r_B^2 + 2r_B r_D \cos\left[\delta_B - \delta_D - \gamma\right], \tag{2.14c}$$
$$\Gamma(B^+ \to D(\to f)K^+) \propto r_D^2 + \ r_B^2 + 2r_B r_D \cos\left[\delta_B - \delta_D + \gamma\right]. \tag{2.14d}$$

The processes in Eqs. (2.14a) and (2.14b) are *CP*-conjugate and it is clear how, in the general case where $\delta_B + \delta_D \neq 0$, a non-zero value of γ leads to *CP* violation in the form of differing decay rates. The same is true for the processes in Eqs. (2.14c) and (2.14d). Depending on the choice of D final state, these expressions can be used to relate γ to various observables that are experimentally accessible. This thesis concerns the choice $f = K^0_S\pi^+\pi^-$ or $f = K^0_S K^+ K^-$, where the terms related to the D decay all have a non-trivial variation over the phase space of the decay. However, it is useful to first analyse the simpler case where f is a two-body state.

The simplest case is when f is chosen to be a *CP* eigenstate, so that $f = \pm\bar{f}$ and the rate equations of (2.14a)–(2.14d) simplify, because $r_D = 1$ and $\delta_D \in \{0, \pi\}$. Measurements of γ in such decay modes are denoted GLW measurements, after Gronau, London, and Wyler who described the approach in the early 90ies [43, 44]. Experimentally it is preferable to measure yield ratios rather than absolute rates, and the observables of interest are thus the *CP* asymmetry

$$\begin{aligned} A_{CP=\pm1} &= \frac{\Gamma[B^- \to D_{CP}K^-] - \Gamma[B^+ \to D_{CP}K^+]}{\Gamma[B^- \to D_{CP}K^-] + \Gamma[B^+ \to D_{CP}K^+]} \\ &= \frac{\pm r_B \sin\delta_B \sin\gamma}{1 + r_B^2 \pm 2r_B \cos\delta_B \cos\gamma}, \end{aligned} \tag{2.15a}$$

as well as the ratio

$$\begin{aligned} R_{CP=\pm1} &= 2\frac{\Gamma[B^- \to D_{CP}K^-] + \Gamma[B^+ \to D_{CP}K^+]}{\Gamma[B^- \to D^0K^-] + \Gamma[B^+ \to \bar{D}^0K^+]} \\ &= 1 + r_B^2 \pm 2r_B \cos\delta_B \cos\gamma. \end{aligned} \tag{2.15b}$$

In practice, A_{CP} and R_{CP} are obtained from measured yield ratios that are corrected with appropriate branching fractions. A measurement of A_{CP} and R_{CP} alone is not sufficient to determine the underlying physics parameters (γ, r_B, δ_B) and this is not solely due to the number of parameters exceeding the number of constraints:

the equations also allow for multiple, ambiguous solutions for $(\gamma$. One way to break the ambiguity, first noted in the original paper [43], is to make further measurements in add nal B decays. These can be described with the formalism described above, but will not share the same ambiguous solutions because (r_B, δ_B) are unique to a given B decay. Another method is to analyse D decay final states that are not CP eigenstates.

A few years later, Atwood, Dunietz, and Sonis analysed an alternative choice of D final states: a simultaneous analysis of a Cabibbo-favoured (CF) decay $D^0 \to f$ and the doubly-Cabibbo-suppressed (DCS) decay $D^0 \to \bar{f}$ into the CP conjugate final state [45, 46]. Their suggested method is named the ADS method after the authors. The classical example is to take $f = K^-\pi^+$ and $\bar{f} = \pi^-K^+$. The relative suppression means that the r_D of Eq. (2.14) is small, typically of the same order of magnitude as r_B, and thus the CP asymmetry of the suppressed decay is $\mathcal{O}(1)$:

$$\begin{aligned} A_{ADS(\bar{f})} &= \frac{\Gamma[B^- \to D(\to \bar{f})K^-] - \Gamma[B^+ \to D(\to f)K^+]}{\Gamma[B^- \to D(\to \bar{f})K^-] + \Gamma[B^+ \to D(\to f)K^+]} \\ &= \frac{r_D r_B \sin(\delta_B - \delta_D)\sin\gamma}{r_D^2 + r_B^2 + 2r_D r_B \cos(\delta_B - \delta_D)\cos\gamma}. \end{aligned} \tag{2.16a}$$

The large CP asymmetry is a prime feature of the ADS method. However, also the suppressed-to-favoured yield ratio is sensitive to the physics parameters of interest:

$$\begin{aligned} R_{ADS(\bar{f})} &= \frac{\Gamma[B^- \to D(\to \bar{f})K^-] + \Gamma[B^+ \to D(\to f)K^+]}{\Gamma[B^- \to D(\to f)K^-] + \Gamma[B^+ \to D(\to \bar{f})K^+]} \\ &= \frac{r_B^2 + r_D^2 + 2r_D r_B \cos(\delta_B - \delta_D)\cos\gamma}{1 + r_D^2 r_B^2 + 2r_D r_B \cos(\delta_B + \delta_D)\cos\gamma}. \end{aligned} \tag{2.16b}$$

The interpretation of A_{ADS} and R_{ADS} in terms of (γ, r_B, δ_B) requires knowledge of the r_D and δ_D parameters, but these can be measured independently. In general, the constraints from a single set of ADS observables suffer the same ambiguities as in the GLW case. However, unlike the GLW case, each D decay mode provides an independent set of constraints, because the parameters related to the D decay vary.

The discussion of this section has centred on the classical case of $B^\pm \to DK^\pm$ decays with a two-body D final state. With minor modifications the techniques have been used to make measurements of γ in B^0 decays [**?**], with B decay final states including excited D mesons [**?**], excited kaons [**?**], or pions [**?**]. The decay $B^\pm \to D\pi^\pm$ also is also CP-violating, although the effect is much smaller than in the $B^\pm \to DK^\pm$ decay, because it expected that $r_B^{D\pi^\pm} \simeq 0.005$ [47], whereas $r_B^{DK^\pm} \simeq 0.1$. Furthermore, it is possible to use multi-body D final states. However, in some cases, a better precision can then be obtained by exploiting phase-space dependent decay rates. This is the topic of the next section.

2.3 Measuring γ using multi-body D final states

In multi-body D decays, the r_D and δ_D parameters of the fundamental rate equations in Eq. (2.14) vary over the phase space of the D decay. This section describes a model-independent approach to measure γ in $B \to D(\to K^0_S\pi^+\pi^-)$ decays by exploiting this variation. The theory is identical for $D \to K^0_S K^+ K^-$ decays, and similar ideas have been proposed for the $D \to K^0_S\pi^+\pi^-\pi^0$ [48] and $D \to 2\pi^+2\pi^-$ modes [49]. First, however, the formalism for describing amplitudes of multi-body decays is briefly reviewed.

2.3.1 Dalitz plots and the phase space of multi-body decays

In general, the phase space of the n-body decay $P \to p_1 + p_2 + ... + p_n$ consists of n four momenta, with a total of $4n$ components. The requirement that each of the final state particles is on-shell provides n constraints on these components, and energy-momentum conservation removes a further 4 degrees of freedom. If the original particle P is s *scalar*, the decay is isotropic, which removes an additional 3 degrees of freedom, leaving the total number of degrees of freedom at $3n-7$. For the specific case of three-body decays, the available phase space can thus be parameterised with only two parameters. A practical and often used choice is the invariant masses

$$s_{12} = m^2(p_1p_2) = (p_1^\mu + p_2^\mu)^2, \qquad s_{13} = m^2(p_1p_3) = (p_1^\mu + p_3^\mu)^2. \tag{2.17}$$

The choice of particle pairs is arbitrary, and the coordinates easily related

$$m_P^2 + m_{p_1}^2 + m_{p_2}^2 + m_{p_3}^2 = m^2(p_1p_2) + m^2(p_1p_3) + m^2(p_2p_3). \tag{2.18}$$

A scatter plot of (s_{12}, s_{13}) values for a sample of particle decays is denoted a Dalitz plot [50]. It has the very useful feature that the presence of (narrow) resonances in the decay leads to visible bands in the scatter plot. Figure 2.4 illustrates how the limits of the Dalitz plot are defined by kinematic constraints, and shows an example of a Dalitz plot for $D \to K^0_S\pi^+\pi^-$ decays in which the $K^*(892)^\pm$ and $\rho(770)$ resonances are clearly visible. The plot shows the sample of $B^+ \to D\pi^+$ decays used to make the measurement described in Chapter 5 and thus the D meson is in a superposition of D^0 and $\overline{D}^0$ states (as detailed in the following section).

In terms of the coordinates of Eq. (2.17) the differential decay rate is given by

$$\mathrm{d}\Gamma = \frac{1}{32(2\pi)^3 m_P^3}|\mathcal{M}|^2\,\mathrm{d}s_{12}\mathrm{d}s_{13}, \tag{2.19}$$

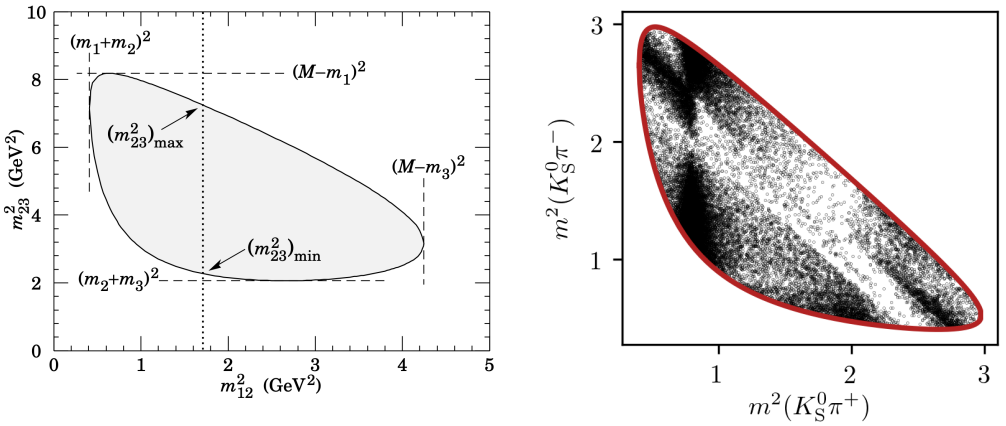

Figure 2.4: (Left) Schematic of a Dalitz plot and the limits of the kinematically allowed phase space limits. (Right) Example of a Dalitz plot for $D \to K^0_S\pi^+\pi^-$ decays where the D meson originates in a $B^+ \to D\pi^+$ decay; the decaying D meson is in a superposition of the D^0 and $\overline{D}^0$ states, but predominantly $\overline{D}^0$-like.

where $\mathcal{M}$ is the QFT matrix element, or total decay amplitude, corresponding to the decay. In general, it is not possible to calculate $\mathcal{M}$ from first principles. Instead, a model is defined with an empirically well motivated form, in which a number of free parameters must be determined experimentally. The simplest case is that of an *isobar* model, where it is assumed that the full decay can be decomposed into consecutive two-body decays of the form $P \to R_{12}(\to p_1 + p_2)p_3$. Thus, $\mathcal{M}$ is expressed as a non-resonant constant amplitude term, k_{NR}, plus a sum of resonance terms

$$\mathcal{M}(s_{12}, s_{13}) = k_{NR} + \sum_r k_r \mathcal{M}^r(s_{12}, s_{13}). \tag{2.20}$$

The exact form of the $\mathcal{M}^r$ function depends on the resonance in question. An overview is given in the PDG review on resonances and references therein [31]. The isobar formalism breaks down when resonances in the decay are not well separated. In this case, models of the form in Eq. (2.20) can still be employed, if the contribution from overlapping resonances are collected in a single term. An example of such a model, is the amplitude model for $D^0 \to K^0_S\pi^+\pi^-$ decays developed by the Belle collaboration for a measurement of the CKM angle β in 2018 [51]. In this model, individual terms are included for $D^0 \to K^*(\to K^0_S\pi^\pm)\pi^\mp$ decays, whereas the $\pi\pi$ and $K\pi$ S-wave contributions are modelled with the so-called K-matrix- and LASS formalisms [52, 53]. The amplitude and phase of $\mathcal{M}$ as predicted by this model are shown in Fig. 2.5.

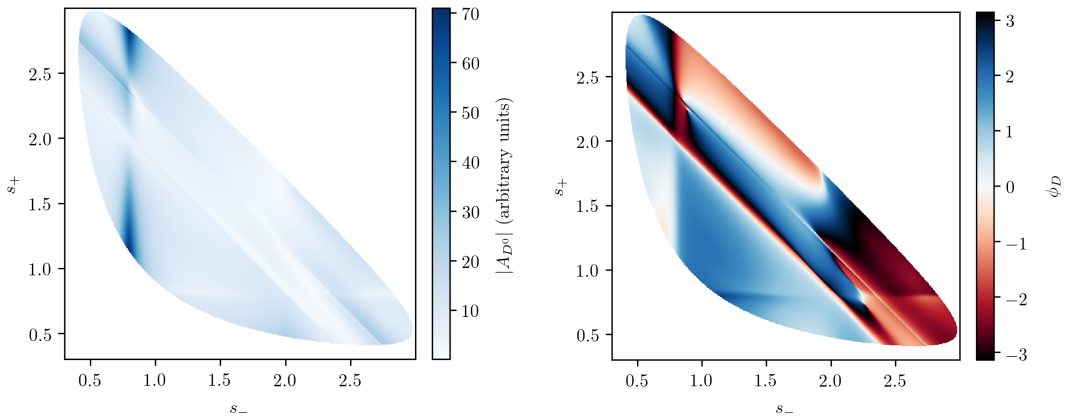

Figure 2.5: The (left) magnitude and (right) phase of the $D \to K^0_S\pi^+\pi^-$ amplitude in the Belle 2018 model [51].

2.3.2 The GGSZ method to measure γ

The non-trivial phase-space dependence of the $D \to K^0_S\pi^+\pi^-$ decay amplitude can be exploited to measure γ with $B^\pm \to DK^\pm$ or $B^\pm \to D\pi^\pm$ decays. This approach was proposed independently by Bondar [54], and by Giri, Grossman, Soffer, and Zupan [55] after whom it takes the commonly used acronym GGSZ. For this specific decay s_- and s_+ are used to described the Dalitz coordinates $m^2(K^0_S\pi^-)$ and $m^2(K^0_S\pi^+)$, respectively, and the D decay amplitude is a function of these coordinates

$$A_S^{(\overline{D})}(s_-, s_+) = A(\overline{(D)}^0 \to K^0_S\pi^+\pi^-). \tag{2.21}$$

To a good approximation the K^0_S meson is a *CP* eigenstate, meaning that the $K^0_S\pi^+\pi^-$ state is self-conjugate. Assuming this approximation to be exact, and that *CP* violation in the D decay is negligible, the D decay amplitude satisfies the symmetry relation

$$A_S^{\overline{D}}(s_-, s_+) = A_S^{D}(s_+, s_-). \tag{2.22}$$

The impact of the K^0_S meson *not* being an exact *CP* eigenstate is treated in detail in Chapter 4. In order to simplify equations, the short-hand notation

$$(s_{-+}) = (s_-, s_+), \qquad (s_{+-}) = (s_+, s_-) \tag{2.23}$$

will be employed for the remainder of the thesis, so that the relation in Eq. (2.22) can be expressed as $A_S^{\overline{D}}(s_{-+}) = A_S^{D}(s_{+-})$. Thus, the rate equations of Eq. (2.14)

for the $D \to K^0_S\pi^+\pi^-$ decay mode are

$$\begin{aligned}
\mathrm{d}\Gamma^-(\mathrm{s}_{-+}) \propto |\mathcal{A}^-_S|^2 &= |A_B|^2|A_{K^0_S}|^2 \\
&\times \Big[|A^D_S(s_{-+})|^2 + r_B^2|A^D_S(s_{+-})|^2 + 2r_B|A^D_S(s_{-+})||A^D_S(s_{+-})| \\
&\times (\cos[\delta_D(s_{-+})]\cos[\delta_B - \gamma] + \sin[\delta_D(s_{-+})]\sin[\delta_B - \gamma])\Big]\,, \quad (2.24a) \\
\mathrm{d}\Gamma^+(\mathrm{s}_{-+}) \propto |\mathcal{A}^+_S|^2 &= |A_B|^2|A_{K^0_S}|^2 \\
&\times \Big[|A^D_S(s_{+-})|^2 + r_B^2|A^D_S(s_{-+})|^2 + 2r_B|A^D_S(s_{-+})||A^D_S(s_{+-})| \\
&\times (\cos[\delta_D(s_{-+})]\cos[\delta_B + \gamma] - \sin[\delta_D(s_{-+})]\sin[\delta_B + \gamma])\Big]\,. \quad (2.24b)
\end{aligned}$$

Here, $\delta_D(s_{-+}) = \phi_D(s_{-+}) - \phi_D(s_{+-}) = -\delta_D(s_{+-})$, where $\phi_D(s_{-+})$ denotes the complex phase of the $A^D_S(s_{-+})$ amplitude, and a standard trigonometric relation have been employed to factorise the terms depending on the complex phases of the B and D decays. It can be seen that in the case where $\gamma = 0$ the B^+ and B^- decay rates are symmetric if the Dalitz coordinates are exchanged: $\Gamma^+(s_-, s_+) = \Gamma^-(s_+, s_-)$. The presence of CP violation in the B decay breaks the symmetry. Therefore it is possible to measure γ (and the nuisance parameters r_B and δ_B) from the phase-space distribution of $B^\pm \to D(\to K^0_S\pi^+\pi^-)K^\pm$ decays, given knowledge of $A^D_S(s_{-+})$.

A series of measurements of γ have been made that use amplitude models of the D decay [56–63]. However, a model-independent approach has been proposed by Bondar and Poluektov [64, 65] that relies on binning phase-space, in which case the necessary information on the D decay amplitude can be summarised in a small set of coefficients that can be measured in a separate experiment. That is the approach followed in this thesis, and has been used previously by the Belle [66] and LHCb collaborations [67]. It is described in detail in the following section.

Such a model-independent approach is favourable for two reasons. Firstly, uncertainty estimates related to model inputs and the choice of parameterisation in an amplitude model are non-trivial, yet would become the leading systematic with the very high precision expected for γ measurements in the near future. Secondly, amplitude models are notoriously hard to reproduce, and in a high-precision era it is favourable that any experiment is easy to reinterpret in various extensions of the SM. This is a lot easier for an experiment that measures a small set of well-defined observables, than for an experiment that fits a complicated amplitude model.

An alternative model-independent approach has recently been proposed by Poluektov [] where the externally measured input on the D-decay phase are Fourier expansion coefficients, and which therefore avoids binning phase space; this approach may have the potential to improve the obtainable precision in the future.

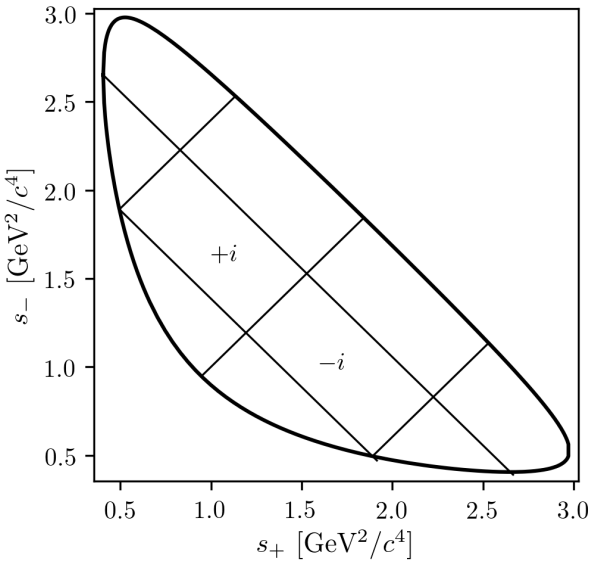

Figure 2.6: Illustration of the binning scheme used in GGSZ measurements: the bins are symmetric around the $m^2(K^0_S\pi^+) = m^2(K^0_S\pi^-$ diagonal, and numbered so that opposite bins have the same number, but with opposite sign.

2.3.3 A model-independent approach

The phase-space distribution can be analysed in a model-independent way, if the D-decay phase space is split into regions, or b[illegible]an the B decay yield in each bin determined experimentally. A measurement of γ using this approach is the main topic of the thesis. This section describes the fundamental principle, whereas the details pertaining to the exact experimental approach are delegated to Section 2.4.

The amplitude symmetry of Eq. (2.22) is exploited by defining $2N$ bins to be symmetric symmetric around the $s_- = s_+$ diagonal of the Dalitz plot, numbered $i = -N$ to N (omitting zero) such that if the point (s_-, s_+) is in bin i, then (s_+, s_-) is in bin $-i$, and by convention $i > 0$ for bins where $s_- > s_+$. The principle is illustrated in Fig. 2.6, but the binning schemes used in actual measurements are more complicated. The decay rates in Eq. (2.24a) can be integrated over such bins, and give the bin yields

$$\begin{aligned} N_i^- &\propto h^- \left[K_i + r_B^2 K_{-i} + 2\sqrt{K_i K_{-i}}\,(c_i x_- + s_i y_-)\right], \\ N_i^+ &\propto h^+ \left[K_{-i} + r_B^2 K_i + 2\sqrt{K_i K_{-i}}\,(c_i x_+ - s_i y_+)\right], \end{aligned} \tag{2.25}$$

where the parameters describing the B decay have been expressed in terms of the observables

$$x_\pm = r_B \cos(\delta_B \pm \gamma), \qquad y_\pm = r_B \sin(\delta_B \pm \gamma), \tag{2.26}$$

and a number of phase-space integrated quantities related to the D-decay have been introduced. The K_i parameters denote fractional yield of a flavour-tagged D^0 decaying into bin i, defined as

$$K_i = \frac{1}{N_K}\int_i \mathrm{d}s^2 |A_{\mathrm{S}}^D(s_{-+})|^2, \qquad N_K = \int \mathrm{d}s^2 |A_{\mathrm{S}}^D(s_{-+})|^2, \tag{2.27}$$

where $\int_i \mathrm{d}s^2$ denotes integration over bin i of the Dalitz plot. The c_i and s_i denote the amplitude-weighted average of $\cos\delta_D(s_{-+})$ and $\sin\delta_D(s_{-+})$ over bin i

$$\begin{aligned} c_i &= \frac{\int_i \mathrm{d}s^2 |A_{\mathrm{S}}^D(s_{-+})||A_{\mathrm{S}}^D(s_{+-})|\cos[\delta_D(s_{-+})]}{\sqrt{\int_i \mathrm{d}s^2 |A_{\mathrm{S}}^D(s_{-+})|^2}\sqrt{\int_i \mathrm{d}s^2 |A_{\mathrm{S}}^D(s_{+-})|^2}}, \\ s_i &= \frac{\int_i \mathrm{d}s^2 |A_{\mathrm{S}}^D(s_{-+})||A_{\mathrm{S}}^D(s_{+-})|\sin[\delta_D(s_{-+})]}{\sqrt{\int_i \mathrm{d}s^2 |A_{\mathrm{S}}^D(s_{-+})|^2}\sqrt{\int_i \mathrm{d}s^2 |A_{\mathrm{S}}^D(s_{+-})|^2}}. \end{aligned} \tag{2.28}$$

By the symmetry properties of $\delta_D(s_{-+})$ these parameters satisfy $c_i = c_{-i}$ and $s_i = -s_{-i}$. The normalisation constants h^+ and h^- are identical in the ideal case, but it is convenient to define them separately for practical reasons: depending on the experimental setup, there may be overall production and detection asymmetries that affect the total signal yields. An experimental analysis can be made insensitive to these effects because they can be absorbed into the normalisation constants, as long as they are constant over the D-decay phase space. This comes at the cost that the information on $x_\pm$ and $y_\pm$ from the overall CP asymmetry is lost, but Section 2.3.5 will show the loss in precision to be minimal.

Thus, for a set of $2N$ bins, the bin yields of Eqs. (2.25) provide $4N$ constraints on a total of $4N + 6$ parameters: $(h^\pm, K_i, c_i, s_i, x_\pm, y_\pm)$. However, the K_i, c_i, and s_i parameters relate only to the D decay, and can thus, in principle, be measured in independent experiments. With such external inputs, a measurement of the $B^\pm \to D(\to K^0_{\mathrm{S}}\pi^+\pi^-)K^\pm$ yields in a set of bins can be used to constrain $x_\pm$ and $y_\pm$, and thereby (γ, r_B, δ_B). The measurement presented in this thesis determines the K_i parameters directly, but uses externally measured values of c_i and s_i as input, as measured in quantum correlated D decays by the CLEO [68] and BESIII [69] collaborations. Because these measurements are the foundation of the approach, they are described in some detail in the following section. In the future, it is possible that the c_i and s_i parameters may be measured in quantum-correlated D decays in LHCb [70], and in charm-mixing measurements [71].

2.3.4 Measuring strong-phase inputs at charm factories

The strong-phase parameters c_i and s_i have been measured by the CLEO and BESIII collaborations, using quantum correlated $D^0\overline{D}^0$ pairs from decays of the $\psi(3770)$ resonance state, itself produced in e^+e^- collisions at the resonance energy. The $\psi(3770)$ has quantum-number $C = -1$, which is conserved in the strong decay into two D mesons, and thus the two D mesons are produced in an anti-symmetric wave function. By observing the decay of one D meson into a specific final state, say a CP eigenstate, the quantum state of the other D meson can be determined. The measurement is based on decays where both D decays are reconstructed, one in the $K^0_S\pi^+\pi^-$ final state, the other in one of several different tag categories. The main principles are outlined below, but most experimental considerations and implementation details are left out for the sake of brevity.

The simplest case is when one D meson decays into a final state that uniquely tags the flavour, such as $\overline{D}^0 \to K^+e^-\bar{\nu}_e$. In that case, the D meson decaying to $K^0_S\pi^+\pi^-$ is known to be in the D^0 state and the decay rate is simply determined by $A^D_S : \Gamma(s_{-+}) \propto |A^D_S(s_{-+})|^2$. This allows for a measurement of the K_i parameters.

If one D meson is reconstructed in a CP-even state, eg. K^+K^-, or a CP-odd state, eg. $K^0_S\pi^0$, the D meson decaying to $K^0_S\pi^+\pi^-$ is known to be in a state of opposite CP. Thus, for a tag-decay of $CP = \pm 1$ the decay rate has the form

$$\Gamma_{CP=\pm1} \propto \left|A^D_S(s_{-+}) \mp A^D_S(s_{+-})\right|^2 \tag{2.29a}$$

and the bin yields will be given by

$$M^\pm_i \propto K_i + K_{-i} \mp 2\sqrt{K_iK_{-i}}c_i. \tag{2.29b}$$

Thus a simultaneous analysis of flavour and CP tagged decays allow for a determination of the K_i and c_i parameter sets.

Finally, the case where both D mesons, for now denoted D and D', decay into the $K^0_S\pi\pi$ final state can be considered. The total amplitudes have contributions from the case where D is in the D^0 state and D' is in the $\overline{D}^0$ state, as well as the opposite flavour assignment. Thus the decay rate satisfies

$$\Gamma_{CP=\pm1} \propto \left|A^D_S(s_{-+})A^D_S(s'_{+-}) + A^D_S(s_{+-})A^D_S(s'_{-+})\right|^2 \tag{2.30a}$$

where s_{-+} denotes the Dalitz-plot coordinates of the D meson, and s'_{-+} those of the D' meson. Defining M_{ij} to be the yield of decays where the D decay is in bin i and the D' in bin j, the bin yields satisfy

$$M_{ij} \propto K_iK_{-j} + K_jK_{-i} - 2\sqrt{K_iK_{-i}K_jK_{-j}}\,(c_ic_j + s_is_j)\,. \tag{2.30b}$$

Thus, analysing these decays in addition to the *CP* and flavour tagged decays provide information on all of K_i, c_i, and s_i. Note, however, that Eqs. (2.29) and (2.30) are invariant under the transformation $\delta_D \to -\delta_D$. In practice, the analysis is extended in a number of ways to enhance the statistics: using "flavour-tag" states that are not exact flavour tags, such as $K^-\pi^+$ [illegible]g self-conjugate multi-body D-decay final states that are not exact *CP* eigen[illegible]s, such as $\pi^+\pi^-\pi^0$, and using the $K^0_L\pi^+\pi^-$ final state as well. However, the main principles are the same as described above.

Where exactly is this phase sign know from? Is the overall sign not arbitrary in amplitude models?

The measurements of c_i and s_i are made for a range of different binning schemes. It was noted already in Ref. [65] that a rectangular binning scheme, such as the examp[illegible] Fig. 2.6, does not provide the optimal sensitivity to γ. A better sensitivity can be obtained if the bins are defined such that δ_D is approximately constant over a given bin, by defining bin i out of N via the conditio[illegible]

$$\text{bin}_i = \{(s_-, s_+) \quad | \quad 2\pi(i - 3/2)/N \; < \; \delta_D(s_-, s_+) \; < \; 2\pi \times (i - 1/2)/N\} \,. \quad (2.31)$$

In practice, the binning scheme is defined by splitting the D-decay phase-space into quadratic *micro bins* with a width of 0.0054 $(\text{GeV}/c^2)^2$ and assigning a bin number to each micro bin via the condition in (2.31) as evaluated in an amplitude model of choice. The obtained binning scheme when using an amplitude model developed by the BaBar collaboration in 2008 [57] is shown in Fig. 2.7a. In Ref [65] it was also shown that the binning can be even further optimised for sensitivity. The suggested figure of merit is

$$Q^2 = \frac{\sum_i \left(\frac{1}{\sqrt{N_i^B}} \frac{\mathrm{d}N_i^B}{\mathrm{d}x}\right)^2 + \left(\frac{1}{\sqrt{N_i^B}} \frac{\mathrm{d}N_i^B}{\mathrm{d}y}\right)^2}{\int \mathrm{d}s^2 \left[\left(\frac{1}{|\Gamma^B(s_{-+})|} \frac{\mathrm{d}|\Gamma^B(s_{-+})|^2}{\mathrm{d}x}\right)^2 + \left(\frac{1}{|\Gamma^B(s_{-+})|} \frac{\mathrm{d}|\Gamma^B(s_{-+})|^2}{\mathrm{d}y}\right)^2\right]} \quad (2.32)$$

which quantifies the statistical sensitivity for a given binning, relative to the one achievable in an unbinned analysis. The CLEO collaboration defined an *optimal* binning scheme by an iterative procedure where, starting from the equal binning scheme, a micro-bin is randomly reassigned new bin numbers in each step, and a step accepted if Q^2 increases. The optimisation is done for the case where $x = y = 0$ and thus Q^2 simplifies to $Q^2_{x=y=0} = \sum_i N_i^{x=y=0}(c_i^2 + s_i^2)/N_{total}^{x=y=0})$. The resulting binning scheme is shown in Fig. 2.7b. An additional binning scheme is defined, denoted the *modified optimal* scheme and shown in Fig. 2.7c, where the Q^2 figure of merit is modified to take into account the presence of backgrounds [68]. The modified optimal binning scheme has proven beneficial to use in measurements with small signal yields [], but is not employed in the present thesis.

Table 2.1: The experimentally measured c_i and s_i values used in the thesis. The $D \to K^0_S\pi^+\pi^-$ values are the combined values from the BESIII and CLEO measurements published by BESIII [69]. The $D \to K^0_S K^+K^-$ values are measured by CLEO [68].

Optimal binning scheme: $D \to K^0_S\pi^+\pi^-$		
Bin i	c_i	s_i
1	-0.037 ± 0.049	0.829 ± 0.097
2	0.837 ± 0.067	0.286 ± 0.152
3	0.147 ± 0.066	0.786 ± 0.154
4	-0.905 ± 0.021	0.079 ± 0.059
5	-0.291 ± 0.041	-1.022 ± 0.062
6	0.272 ± 0.082	-0.977 ± 0.176
7	0.918 ± 0.017	-0.184 ± 0.065
8	0.773 ± 0.033	0.277 ± 0.118

2-bins binning scheme: $D \to K^0_S K^+K^-$		
Bin i	c_i	s_i
1	0.818 ± 0.107	-0.445 ± 0.215
2	-0.746 ± 0.083	-0.229 ± 0.220

Both the CLEO and BESIII collaborations have measured the values of c_i and s_i for the equal, optimal, and modified optimal binning schemes. The results are also shown in Fig. 2.7, where they are compared to the expectation from the latest amplitude model [51]. The measurements presented in this thesis are based on a combination of the BESIII and CLEO results for the optimal binning scheme, made by the BESIII collaboration [69] and tabulated in Table 2.1.

While the *definition* and *optimisation* of these binning schemes depend on knowledge of $A^D_S(s_-, s_+)$ via an amplitude model, it is important to note that no model information is needed when the binning schemes are used in the subsequent measurements of strong-phases[5] or *CP*-observables. Therefore the measurements will not be biased by any modelling imperfections, although the obtained precision might be lower than expected.

The preceding discussion has been focusing on the $D \to K^0_S\pi^+\pi^-$ channel, however the $D \to K^0_S K^+K^-$ channel can be analysed completely analogously. The CLEO collaboration measure c_i and s_i values for this mode as well, in three binning schemes [68]. These are all equal-phase binning schemes, with 2, 3, and 4 bins,

[5]With the exception of minimal model-dependence introduced when the $K^0_L\pi^+\pi^-$ final state is employed to constrain the s_i parameters by the D-factories [68, 69], the impact of which is well under control.

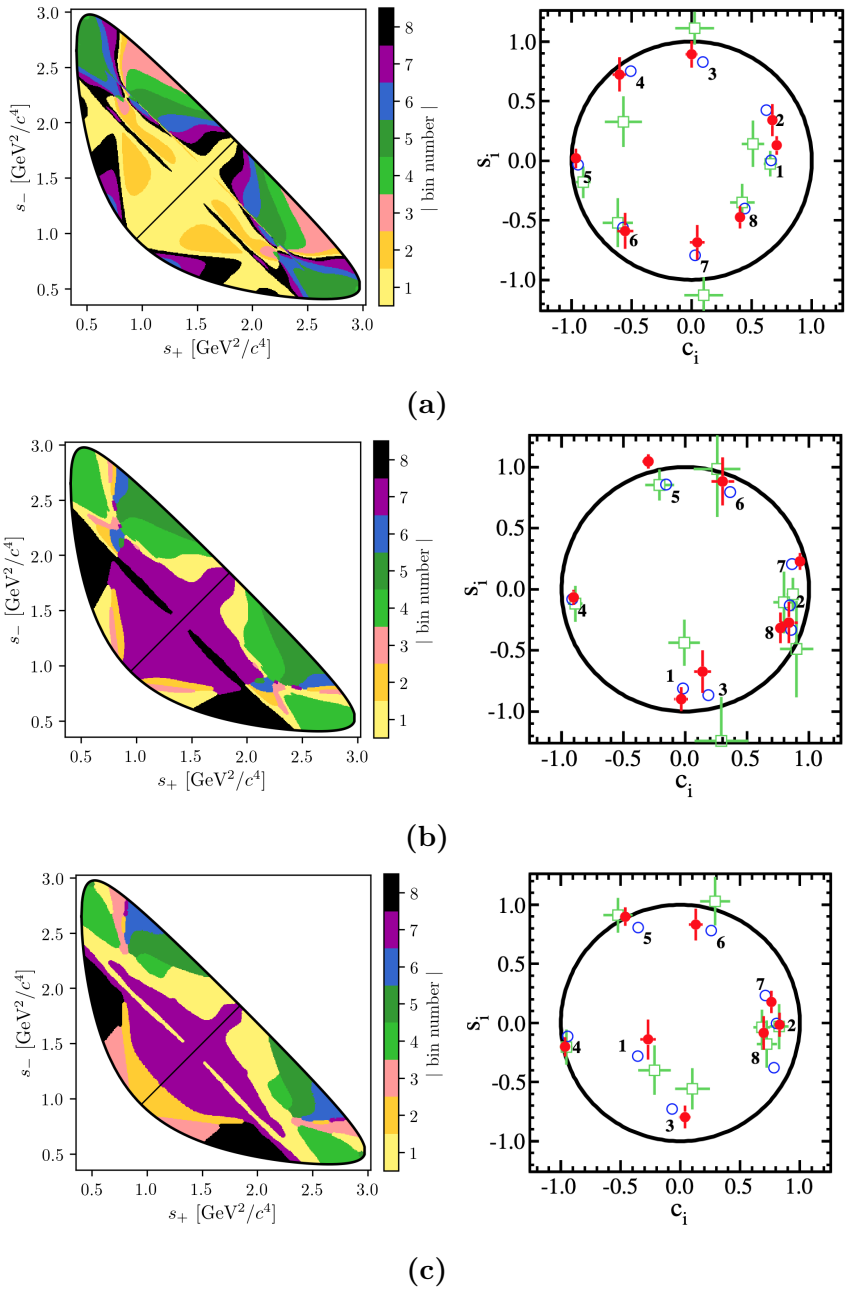

Figure 2.7: The (left) binning schemes and (right) measured values of (c_i, s_i) for (a) equal, (b) optimal, and (c) modified optimal binning schemes for $D \to K^0_S\pi^+\pi^-$. The plots of the measured values are taken from Ref. [69] and show the results obtained by (red) BESIII, (green) CLEO, and (blue) the model expectation using the model from Ref. [51]. The measurement featured in this thesis used the optimal binning scheme.

respectively, shown in Fig. 2.8. The $D \to K^0_S K^+ K^-$ decay amplitude is almost completely dominated by two K^+K^- resonances, the *CP*-odd $\phi(1020)$ and the *CP*-even $a_0(980)$, and this means that very little gain in sensitivity can be made by altering the equal-phase binning schemes. The measured c_i and s_i values are also shown in Fig. 2.8 and tabulated in Table 2.1 for the 2-bins scheme, which is used in this thesis. A BESIII measurement is in preparation, but has not been finished at the time of writing.

2.3.5 Global CP asymmetry and the relation to GLW and ADS measurements

The introduction of separate normalisation factors h^+ and h^- in Eq. (2.25) hides the fact that information on γ (in principle) can be obtained from the asymmetry in phase-space-integrated B^+ and B^- yields. In the ideal case where $h^- = h^+$ the total yield asymmetry is

$$\begin{aligned} A_{GGSZ} &= \frac{\sum_i N^-_- - N^+_i}{\sum_{i=-N}^{N} N^- i - + N^+_i} = \frac{\sum_{i=-N}^{N} \sqrt{K_i K_{-i}} c_i (x_- - x_+)}{1 + r_B^2 + 2\sum_{i=-N}^{N} \sqrt{K_i K_{-i}} c_i (x_- + x_+)} \\ &= \frac{2\sum_{i=1}^{N} \sqrt{K_i K_{-i}} c_i (x_- - x_+)}{1 + r_B^2 + 4\sum_{i=1}^{N} \sqrt{K_i K_{-i}} c_i (x_- + x_+)}, \end{aligned} \tag{2.33}$$

where it has been exploited that $\sum_{i=-N}^{N} \sqrt{K_i K_{-i}} s_i = 0$ by definition. The size of the asymmetry is governed by the factor $\sum_{i=1}^{N} \sqrt{K_i K_{-i}} c_i$, which is small for $D \to K^0_S \pi^+ \pi^-$ and $D \to K^0_S K^+ K^-$ decays. The underlying reason is that $\delta_D(s_-, s_+)$ varies significantly across phase-space for these decays, as evident by the spread in the values of c_i in Table 2.1, which reduces the *average* of the asymmetry-generating D^0–$\overline{D}^0$ interference term to being close to zero. The value of $\sum_{i=-N}^{N} \sqrt{K_i K_{-i}} c_i$ is closely related to the *CP* content of the final state in question: for a self-conjugate *CP* even (odd) final state

$$A_{D^0}(s_-, s_+) = {}^{+}_{(-)} A_{\overline{D}^0}(s_-, s_+) = {}^{+}_{(-)} A_{D^0}(s_+, s_-) \tag{2.34}$$

and thus $\sum_{i=1}^{N} \sqrt{K_i K_{-i}} c_i = {}^{+}_{(-)} 1$. This motivates the definition of the *CP*-even fraction of the decay

$$\mathcal{F}_+ \equiv \frac{1}{2} \left(1 + \sum_{i=1}^{N} \sqrt{K_i K_{-i}} c_i \right). \tag{2.35}$$

With $\mathcal{F}_+$ in hand, the asymmetry in Eq. (2.33) can be rewritten

$$A_{GGSZ} = \frac{(2\mathcal{F}_+ - 1) r_B \sin\delta_B \sin\gamma}{1 + r_B^2 (2\mathcal{F}_+ - 1) 2 r_B \cos\delta_B \cos\gamma}, \tag{2.36}$$

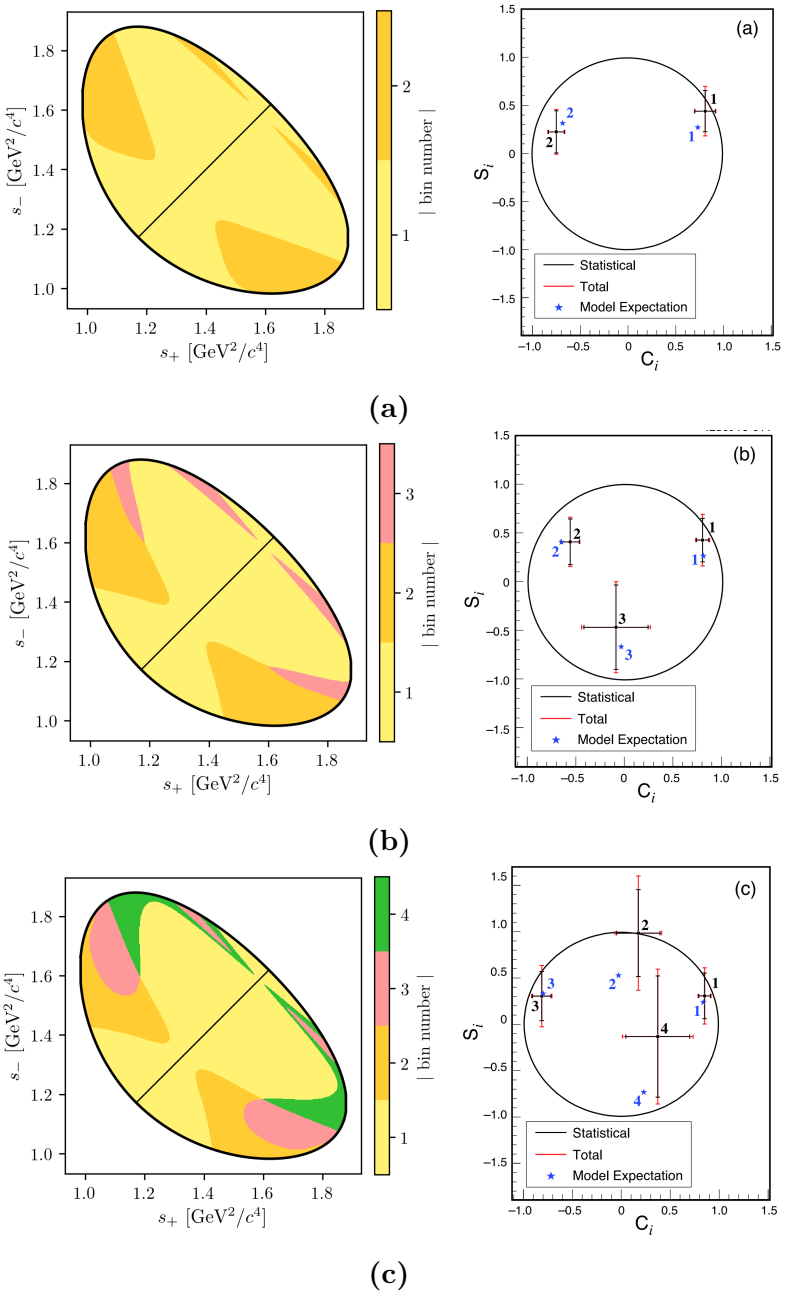

Figure 2.8: The (left) binning schemes and (right) measured values of (c_i, s_i) for the (a) 2-, (b) 3-, and (c) 4-bins binning schemes for $D \to K^0_S K^+ K^-$. The plots of the measured values are taken from Ref. [68] and show the (error bars) results obtained by CLEO, and (blue) the model expectation using the model from Ref. [58]. The measurement featured in this thesis uses the 2-bins scheme.

which is the usual form used in quasi-GLW measurements []; for $N = 1$ the definition in Eq. (2.35) is equivalent to $\mathcal{F}_+$ as defined in Ref. []. The value of $\mathcal{F}_+$ is independent of the number and shape of bins in a given binning scheme, as long as the bin definitions follow the symmetry principles outlined in Section 2.3.3. For $D \to K^0_S\pi^+\pi^-$ and Å decays the values of $\mathcal{F}_+$ are

$$\begin{aligned} \mathcal{F}_+(K^0_S\pi^+\pi^-) &= X? \\ \mathcal{F}_+(K^0_S K^+K^-) &= X? \end{aligned} \tag{2.37}$$

as evaluated with the Belle 2018 model for $D \to K^0_S\pi^+\pi^-$ decays and the BaBar 2010 model for $D \to K^0_S K^+K^-$ decays. Since $r_B^{DK^\pm} \sim 0.1$ the predicted global asymmetries are thus approximately 1–2 %, which is not resolvable with the current experimental yields. As shown in Chapter 4, *CP* violation in the K^0_S sector leads to asymmetries of a similar size, further complicating the use of global asymmetries to constrain $x_\pm$ and $y_\pm$. Thus these modes are ill-suited for quasi-GLW measurements, and ignoring global asymmetries leads to a negligible loss of information on γ in a GGSZ measurement. The reverse is true for a well-suited quasi-GLW mode, such as $D \to \pi^+\pi^-\pi^0$: if $\mathcal{F}_+$ is close to either zero or unity, it means that (c_i, s_i) will be close to $(\pm 1, 0)$ in all bins for *any* given binning scheme, and the set of bins will provide almost identical constraints on $x_\pm$ and $y_\pm$. Thus, the binning of phase space leads to no significant gain in precision compared to a global analysis.

Indeed, a crucial quality of the GGSZ method, is that exactly because each bin-pair provides independent constraints on $x_\pm$ and $y_\pm$, the method provides a single solution for (γ, r_B, δ_B) that does not suffer the ambiguities of the ADS and GLW approaches. In order to illustrate this further, it is useful to make one more comparison of the model-independent GGSZ formalism to the ADS and GLW formalisms. If there was no *CP* symmetry the B^+ yield in bin $+i$ would equal the B^- yield in bin $-i$. Therefore the relevant *CP* asymmetry for a given Dalitz bin is

$$\begin{aligned} A^i_{GGSZ} &\equiv \frac{N^-_i - N^+_{-i}}{N^-_i + N^+_{-i}} \\ &= \frac{\sqrt{K_i K_{-i}}(c_i(x_- - x_+) + s_i(y_- - y_+))}{K_i + r_B^2 K_{-i} + 2\sqrt{K_i K_{-i}}(c_i(x_- + x_+) + s_i(y_- + y_+))}. \end{aligned} \tag{2.38}$$

This expression is identical to the ADS asymmetry in Eq. (2.16a) if the effective D-decay parameters r^i_D and δ^i_D are defined via

$$\kappa_i \cos\delta^i_D \equiv c_i \quad , \quad \kappa_i \sin\delta^i_D \equiv s_i \quad , \quad r^i_D \equiv \sqrt{K_i/K_{-i}}, \tag{2.39}$$

and a coherence factor, κ, is included in the interference terms of the ADS expression, as is standard for multi-body D decays []. These parameters allow us to classify

Table 2.2: Classification of the bins used in model-independent GGSZ measurements, in terms of whether the interplay between the D^0 and $\overline{D}^0$ amplitudes in the bin resemble typical GLW or ADS behaviour. The parameters are calculated using the 2018 Belle model [] for $D \to K^0_S\pi^+\pi^-$ decays and the 2010 BaBar model [] for $D \to K^0_S K^+K^-$ decays.

Optimal binning scheme: $D \to K^0_S\pi^+\pi^-$					
Bin i	$\hat{r}_D$	$\hat{\delta}_D$	$\mathcal{F}_+$	κ	Bin type
1	0.473	91.9°	48.97 %	0.81	Mixed
2	0.164	11.1°	63.38 %	0.85	ADS-like
3	0.157	79.4°	52.50 %	0.89	ADS-like
4	0.768	175.3°	5.85 %	0.92	GLW-odd-like
5	0.759	−99.9°	42.84 %	0.87	Mixed
6	0.223	−64.5°	57.92 %	0.87	ADS-like
7	0.651	−13.3°	89.44 %	0.89	GLW-even-like
8	1.745	21.0°	87.08 %	0.92	GLW-even-like

2-bins binning scheme: $D \to K^0_S K^+K^-$					
Bin i	$\hat{r}_D$	$\hat{\delta}_D$	$\mathcal{F}_+$	κ	Bin type
1	0.816	19.8°	86.14 %	0.78	GLW-even-like
2	0.775	154.5°	16.23 %	0.77	GLW-odd-like

a given pair of bins with number $\pm i$ as either *GLW-like*, if δ^i_D is close to 0 or π and r^i_D is close to unity, or *ADS-like* if $0 < r^i_D \ll 1$. The *CP*-even fraction of the D-decay can also be defined for a given bin-pair:

$$\mathcal{F}^i_+ = \mathcal{F}^{-i}_+ \equiv \frac{1}{2}\left(1 + 2c_i\frac{\sqrt{K_i K_{-i}}}{K_i + K_{-i}}\right) = \frac{1}{2}\left(1 + 2c_i\frac{r^i_D}{1 + {r^i_D}^2}\right). \tag{2.40}$$

A GLW-even-like bin pair will have $\mathcal{F}^i_+ \simeq 1$ and a GLW-odd-like bin pair will have $\mathcal{F}^i_+ \simeq 0$.

Table 2.2 summarises a classification of the bins for the optimal $D \to K^0_S\pi^+\pi^-$ binning scheme and the 2-bins $D \to K^0_S K^+K^-$ binning scheme following these principles. Two bins are classified as *mixed* because r^i_D is not particularly small, but $\mathcal{F}^i_+$ is close to 0.5. The fact that multiple bin types appear for both the $D \to K^0_S\pi^+\pi^-$ and $D \to K^0_S K^+K^-$ modes underline that each mode benefits from being analysed in the GGSZ formalism, and that the bins provide independent constraints, allowing for a non-ambiguous solution for (γ, r_B, δ_B).

2.4 Strategy for the LHCb measurement

The main topic of the thesis is a model-independent GGSZ measurement using $B^\pm \to DK^\pm$ and $B^\pm \to D\pi^\pm$ decays, and the two D final states $K^0_S\pi^+\pi^-$ and $K^0_S K^+K^-$. The measurement uses the optimal binning scheme for the $D \to K^0_S\pi^+\pi^-$ mode, with the combined strong-phase inputs from the BESIII [69] and CLEO [68] collaborations published in Ref. [69]. For the $D \to K^0_S K^+K^-$ channel, the 2-bins scheme is used with the strong-phase parameters measured by the CLEO collaboration [68]. The details of the analysis are presented in Chapter (5), but the overall strategy and a few extensions of the formalism from the previous sections are given here.

Due to the geometry of the LHCb detector, the signal reconstruction efficiency for $B^\pm \to D(\to K^0_S h^+h^-)h'^\pm$ decays varies significantly across the D-decay phase space. Denoting the efficiency profile as $\eta(s_-, s_+)$, the yield equations of Eq. (2.25) are therefore modified slightly

$$\begin{aligned} N_i^- &= h^{B^-}\left[F_i + r_B^2 F_{-i} + 2\sqrt{F_i F_{-i}}\,(c'_i x_- + s'_i y_-)\right], \\ N_i^+ &= h^{B^+}\left[F_{-i} + r_B^2 F_i + 2\sqrt{F_i F_{-i}}\,(c'_i x_+ - s'_i y_+)\right], \end{aligned} \tag{2.41}$$

where the phase-space integrated quantities now include the efficiency profile

$$F_i = \frac{1}{N_F}\int_i \mathrm{d}s^2\,\eta(s_{-+})|A^D_S(s_{-+})|^2, \qquad N_F = \int \mathrm{d}s^2\,\eta(s_{-+})|A^D_S(s_{-+})|^2, \tag{2.42}$$

$$c'_i = \frac{\int_i \mathrm{d}s^2\,\eta(s_{-+})|A^D_S(s_{-+})||A^D_S(s_{+-})|\cos[\delta_D(s_{-+})]}{\sqrt{\int_i \mathrm{d}s^2\,\eta(s_{-+})|A^D_S(s_{-+})|^2}\sqrt{\int_i \mathrm{d}s^2\,\eta(s_{-+})|A^D_S(s_{+-})|^2}}, \tag{2.43}$$

with an analogous definition of s'_i. At leading order, the strong-phase parameters are unaffected by the non-uniform efficiency, and, in addition, the bin definitions favour bins for which c_i and s_i take on similar values across each bin. Therefore, the c_i and s_i values reported by the charm factories are used directly in the measurement. The impact on the obtained central values is negligible, as described in detail in Section 5.4 where a systematic uncertainty is assigned.

The F_i *are* significantly different to the K_i due to the experimental acceptance profile in LHCb. Given external inputs for the strong-phase parameters, it is possible to fit the F_i parameters *and* $x_\pm$ and $y_\pm$ simultaneously in a fit to the LHCb $B^\pm \to DK^\pm$ data set, in which case the obtained F_i parameters incorporate the correct acceptance profile correction by construction. However, the obtainable precision for the *CP* observables measured by this procedure is suboptimal. As

an alternative, the first LHCb measurement [67] made a simultaneous analysis of $B^\pm \to DK^\pm$ and a much larger sample of $B^\pm \to D\pi^\pm$ decays; since the F_i parameters relate to the D decay, they can effectively be obtained in the $D\pi^\pm$ sample and shared between the two $B^\pm \to Dh^\pm$ channels. However, there is *CP* violation present in the $B^\pm \to D\pi^\pm$ decays, which led to a dominant systematic uncertainty. Later LHCb measurements [3, 72] instead relied on flavour tagged D mesons from $\overline{B}^0 \to D^{*+}(\to D^0\pi^+)\mu^-\bar{\nu}_\mu X$ decays to obtain F_i, where no *CP* violation in possible. However, due to necessarily different triggering paths and selections, the acceptance profile is not exactly identical between semi-leptonic decays and the $B^\pm \to Dh^\pm$ decays of interest. An efficiency correction based on simulation was therefore applied to obtain the correct F_i, and in this case, the uncertainty related to the correction constituted the largest systematic uncertainty on the measurement.

Both sources of systematic uncertainty can be avoided by making a simultaneous analysis of $B^\pm \to DK^\pm$ and $B^\pm \to D\pi^\pm$ decays, where *CP*-violating observables are measured in *both* channels and the F_i parameters are shared. Effectively, the F_i are determined in the high statistics $B^\pm \to D\pi^\pm$ channel, but with no systematic effect from *CP*-violation in that channel, since the *CP*-violation is incorporated in the yield description. At the start of the work that lead to this thesis, it was not clear to what degree the measured *CP*-violating observables in $B^\pm \to D\pi^\pm$ decays were affected by *CP* violation in the neutral kaon sector. The impact had been shown to scale as $\mathcal{O}(|\epsilon|/r_B)$ [73], which is negligible for the $B^\pm \to DK^\pm$ channel but suggests potentially large biases in the $B^\pm \to D\pi^\pm$ channel, where r_B is 20 times smaller. However, the dedicated analysis presented in Chapter 4 has proved the effect on GGSZ measurements to be in fact be *smaller* than $\mathcal{O}(|\epsilon|/r_B)$ and the simultaneous measurement is indeed viable.

The measurement is performed by making extended maximum-likelihood fits to the m_B spectra of $B \to D(\to K^0_S h^+h^-)h'^\pm$ candidates split by charge and Dalitz bin. The $B^\pm \to DK^\pm$ signal yields are parameterised using the expressions in Eq. (2.41) directly, thus obtaining values for $x^{DK}_\pm$ and $y^{DK}_\pm$ directly. The Cartesian *CP*-violating observables $x_\pm$ and $y_\pm$ are employed because they lead to better statistical behaviour than fits to data where the underlying parameters $(\gamma, r_B^{DK^\pm}, \delta_B^{DK^\pm})$ are determined [], at the cost of introducing a fourth degree of freedom. With the addition of the $B^\pm \to D\pi^\pm$ mode as a true signal channel, two new underlying parameters are introduced, $r_B^{D\pi^\pm}$ and $\delta_B^{D\pi^\pm}$. It is only necessary to introduce an additional two, not four, Cartesian parameters [74] by defining

$$\xi_{D\pi^\pm} = \left(\frac{r_B^{D\pi^\pm}}{r_B^{DK^\pm}}\right) \exp[i(\delta_B^{D\pi^\pm} - \delta_B^{DK^\pm})] \tag{2.44a}$$

643 and letting

$$x_\xi^{D\pi} = \mathrm{Re}[\xi_{D\pi^\pm}] \qquad\qquad y_\xi^{D\pi} = \mathrm{Im}[\xi_{D\pi^\pm}]. \tag{2.44b}$$

644 In terms of these parameters, the usual Cartesian $x_\pm$ and $y_\pm$ are given by

$$x_\pm^{D\pi} = x_\xi^{D\pi} x_\pm^{DK} - y_\xi^{D\pi} y_\pm^{DK}, \qquad\qquad y_\pm^{D\pi} = x_\xi^{D\pi} y_\pm^{DK} + y_\xi^{D\pi} x_\pm^{DK}. \tag{2.45}$$

645 Using this expression, the $B^\pm \to D\pi^\pm$ yields can also be defined via Eq. (2.41) in the
646 maximum-likelihood fit. This allows for a stable fit for all six x and y parameters, as
647 well as the shared F_i, as described in much greater detail in Chapter 5. Note that ξ
648 does not depend on γ: all information on *CP* asymmetries in both the $B^\pm \to DK^\pm$
649 and $B^\pm \to D\pi^\pm$ channels is encoded in $x_\pm^{DK}$ and $y_\pm^{DK}$.

650 The combined analysis of $B^\pm \to DK^\pm$ and $B^\pm \to D\pi^\pm$ decays presents a sig-
651 nificant step forward, because it solves the problem of obtaining F_i parameters
652 for the appropriate acceptance profile in a manner that avoids leading systematic
653 uncertainties, and almost all reliance on simulation. This is of great importance,
654 if the large data samples that will be collected by LHCb in the future are to be
655 exploited to their full potential.

3

The LHCb experiment

We have a detector? I thought ntuples were made of magic.

3.1 Subdetectors

3.1.1 The VELO

3.1.2 Magnet and tracking stations

3.1.3 The RICH

3.1.4 Calorimeters

3.1.5 Muon detectors

3.2 Track reconstruction

3.3 The LHCb triggerring system

3.3.1 The level-0 hardware trigger

3.3.2 High-level triggers

3.3.3 Offline data filtering: the LHCb stripping

3.4 Simulation

4

Neutral kaon CP violation and material interaction in GGSZ measurements

Will follow paper structure reasonably closely, with added content from full LHCb simulation to verify the simple setup.

5

A GGSZ measurement with $B^{\pm} \to Dh^{\pm}$ decays

First I will return to describing the overall strategy a bit, then one can proceed with the data analysis section

5.1 Candidate selection

5.2 Signal and background components

5.3 Measurement of the CP-violation observables

5.4 Systematic uncertainties

5.5 Obtained constraints on γ

6 Conclusions

Say something clever

Bibliography

[1] LHCb collaboration, R. Aaij *et al.*, *Measurement of the CKM angle γ using $B^\pm \to [K^0_S h^+ h^-]_D h^\pm$ decays*, Submitted to JHEP (2020).

[2] M. Bjørn and S. Malde, *CP violation and material interaction of neutral kaons in measurements of the CKM angle γ using $B^\pm \to DK^\pm$ decays where $D \to K^0_S \pi^+ \pi^-$*, JHEP **19** (2020) 106, arXiv:1904.01129.

[3] LHCb collaboration, R. Aaij *et al.*, *Measurement of the CKM angle γ using $B^\pm \to DK^\pm$ with $D \to K^0_S \pi^+ \pi^-$, $K^0_S K^+ K^-$ decays*, JHEP **08** (2018) 176, Erratum ibid. **10** (2018) 107, arXiv:1806.01202.

[4] E. Noether, *Invariante Variationsprobleme*, Nachrichten von der Gesellschaft der Wissenschaften zu Göttingen, Mathematisch-Physikalische Klasse **1918** (1918) 235.

[5] J. F. Donoghue, E. Golowich, and B. R. Holstein, *Dynamics of the Standard Model*, Cambridge University Press, Cambridge, 2014.

[6] A. D. Sakarov, *Violation of CP Invariance, C Asymmetry, and Baryon Asymmetry of the Universe*, JETP Letters **5** (1966) 24.

[7] G. Luders, *On the Equivalence of Invariance under Time Reversal and under Particle-Antiparticle Conjugation for Relativistic Field Theories*, Kong. Dan. Vid. Sel. Mat. Fys. Med. **28N5** (1954) 1.

[8] C. S. Wu *et al.*, *Experimental Test of Parity Conservation in Beta Decay*, Physical Review **105** (1957) 1413.

[9] T. D. Lee and C. N. Yang, *Question of Parity Conservation in Weak Interactions*, Physical Review **104** (1956) 254.

[10] J. H. Christenson, J. W. Cronin, V. L. Fitch, and R. Turlay, *Evidence for the 2π Decay of the K^0_2 Meson*, Physical Review Letters **13** (1964) 138.

[11] BABAR Collaboration *et al.*, *Observation of CP Violation in the ${\mathit{B}}^{0}$ Meson System*, Physical Review Letters **87** (2001) 091801.

[12] Belle Collaboration *et al.*, *Observation of Large CP Violation in the Neutral B Meson System*, Physical Review Letters **87** (2001) 091802.

[13] K. Abe, *Study of B+- -> D_CP K+- and D*_CP K+- decays*, Physical Review D **73** (2006) 051106, arXiv:hep-ex/0601032.

[14] B. Collaboration *et al.*, *Evidence for Suppressed Decay B- -> DK-, D -> K+pi-*, Physical Review Letters **106** (2011) 231803, arXiv:1103.5951.

[15] T. B. Collaboration and P. d. A. Sanchez, *Measurement of CP observables B+- -> D_CP K+- decays and constraints on the CKM angle gamma*, Physical Review D **82** (2010) 072004, arXiv:1007.0504.

[16] The BABAR Collaboration *et al.*, *Search for $b\ensuremath{\rightarrow}u$ transitions in ${B}^{-}\ensuremath{\rightarrow}D{K}^{-}$ and ${D}^{*}{K}^{-}$ decays*, Physical Review D **82** (2010) 072006.

[17] C. Collaboration, *Measurements of branching fraction ratios and CP asymmetries in B+/- ->D_CP K+/- decays in hadron collisions*, Physical Review D **81** (2010) 031105, arXiv:0911.0425.

[18] C. Collaboration, *Measurements of branching fraction ratios and CP-asymmetries in suppressed B^ -> D(-> K^ pi^)K^ and B^ -> D(-> K^ pi^)pi^ decays*, Physical Review D **84** (2011) 091504, arXiv:1108.5765.

[19] LHCb collaboration, R. Aaij *et al.*, *Observation of CP violation in $B^{\pm} \to DK^{\pm}$ decays*, Phys. Lett. **B712** (2012) 203, Erratum ibid. **B713** (2012) 351, arXiv:1203.3662.

[20] LHCb collaboration, R. Aaij *et al.*, *First observation of CP violation in the decays of B^0_s mesons*, Phys. Rev. Lett. **110** (2013) 221601, arXiv:1304.6173.

[21] LHCb collaboration, R. Aaij *et al.*, *Observation of CP violation in neutral D-meson decays*, LHCb-PAPER-2019-006, in preparation.

[22] K. Abe *et al.*, *Constraint on the matter–antimatter symmetry-violating phase in neutrino oscillations*, Nature **58** (2020) 339.

[23] L. K. Gibbons *et al.*, *Measurement of the CP-violation parameter Re(\ensuremath{\varepsilon}'/\ensuremath{\varepsilon})*, Physical Review Letters **70** (1993) 1203.

[24] G. D. Barr *et al.*, *A new measurement of direct CP violation in the neutral kaon system*, Physics Letters B **317** (1993) 233.

[25] J. R. Batley *et al.*, *A precision measurement of direct CP violation in the decay of neutral kaons into two pions*, Physics Letters B **544** (2002) 97.

[26] KTeV Collaboration *et al.*, *Measurements of direct CP violation, CPT symmetry, and other parameters in the neutral kaon system*, Physical Review D **67** (2003) 012005.

[27] HFLAV, Y. S. Amhis *et al.*, *Averages of b-hadron, c-hadron, and τ-lepton properties as of 2018*, `arXiv:1909.12524`, updated results and plots available at `https://hflav.web.cern.ch/`.

[28] M. Kobayashi and T. Maskawa, *CP-Violation in the Renormalizable Theory of Weak Interaction*, Progress of Theoretical Physics **49** (1973) 652.

[29] N. Cabibbo, *Unitary Symmetry and Leptonic Decays*, Physical Review Letters **10** (1963) 531.

[30] L.-L. Chau and W.-Y. Keung, *Comments on the Parametrization of the Kobayashi-Maskawa Matrix*, Physical Review Letters **53** (1984) 1802.

[31] Particle Data Group, M. Tanabashi *et al.*, *Review of particle physics*, Phys. Rev. **D98** (2018) 030001, and 2019 update.

[32] L. Wolfenstein, *Parametrization of the Kobayashi-Maskawa Matrix*, Physical Review Letters **51** (1983) 1945.

[33] Y. H. Ahn, H.-Y. Cheng, and S. Oh, *Wolfenstein parametrization at higher order: Seeming discrepancies and their resolution*, Physics Letters B **703** (2011) 571.

[34] A. J. Buras, M. E. Lautenbacher, and G. Ostermaier, *Waiting for the top quark mass, $\{\mathit{K}\}\hat{}\{+\}$\ensuremath\{\rightarrow\}$\{\mathrm\{\ensuremath\{\pi\}\}\}\hat{}\{+\}$\ensuremath $\{\mathit\{B\}\}_\{\mathit\{s\}\}\hat{}\{0\}$-B$\{\mathrm\{\ifmmode\bar\else\textasciimacron\fi\}\}_\{\ mixing, and CP asymmetries in B decays*, Physical Review D **50** (1994) 3433.

[35] J. Charles *et al.*, *CP violation and the CKM matrix: Assessing the impact of the asymmetric B factories*, The European Physical Journal C - Particles and Fields **41** (2005) 1.

[36] J. Brod and J. Zupan, *The ultimate theoretical error on γ from $B \to DK$ decays*, Journal of High Energy Physics **2014** (2014) 51.

[37] M. Blanke and A. J. Buras, *Emerging $$\Delta M_\{d\}$$ΔMd-anomaly from tree-level determinations of $$/V_\{cb\}/$$/Vcb/and the angle $$\gamma $$γ*, The European Physical Journal C **79** (2019) 159.

[38] CKMfitter group, J. Charles *et al.*, *Current status of the Standard Model CKM fit and constraints on $\Delta F = 2$ new physics*, Phys. Rev. **D91** (2015) 073007, arXiv:1501.05013, updated results and plots available at http://ckmfitter.in2p3.fr/.

[39] UTfit collaboration, M. Bona *et al.*, *The unitarity triangle fit in the standard model and hadronic parameters from lattice QCD: A reappraisal after the measurements of Δm_s and $BR(B \to \tau\nu_\tau)$*, JHEP **10** (2006) 081, arXiv:hep-ph/0606167, updated results and plots available at http://www.utfit.org/.

[40] E. Kou *et al.*, *The Belle II Physics Book*, Progress of Theoretical and Experimental Physics **2019** (2019) 123C01, arXiv:1808.10567.

[41] LHCb collaboration *et al.*, *Physics case for an LHCb Upgrade II - Opportunities in flavour physics, and beyond, in the HL-LHC era*, arXiv:1808. 08865 [hep-ex] (2019) arXiv:1808.08865.

[42] Y. Grossman and M. Savastio, *Effects of $ \{K\hat{0}\}-\{\{\overline\{K\}\}\hat{0}\} $mixing on determining γ from $B\pm \to DK\pm$*, Journal of High Energy Physics **2014** (2014) 8.

[43] M. Gronau and D. Wyler, *On determining a weak phase from charged B decay asymmetries*, Physics Letters B **265** (1991) 172.

[44] M. Gronau and D. London, *How to determine all the angles of the unitarity triangle from Bd0 → DKs andBs0 → Dϕ*, Physics Letters B **253** (1991) 483.

[45] D. Atwood, I. Dunietz, and A. Soni, *Enhanced CP Violation with $\mathit{B}\ensuremath{\rightarrow}{\mathrm{KD}}\hat{0}({\overline{D}}\hat{0})$ Modes and Extraction of the Cabibbo-Kobayashi-Maskawa Angle $\ensuremath{\gamma}$*, Physical Review Letters **78** (1997) 3257.

[46] D. Atwood, I. Dunietz, and A. Soni, *Improved methods for observing CP violation in ${B}\hat{}\ifmmode\pm\else\textpm\fi{}\ensuremath{\rightarrow}\mathrm{KD}$ and measuring the CKM phase $\ensuremath{\gamma}$*, Physical Review D **63** (2001) 036005.

[47] M. Kenzie, M. Martinelli, and N. Tuning, *Estimating ${r}_{B}\hat{D}\ensuremath{\pi}$ as an input to the determination of the CKM angle $\ensuremath{\gamma}$*, Physical Review D **94** (2016) 054021.

[48] T. Evans, J. Libby, S. Malde, and G. Wilkinson, *Improved sensitivity to the CKM phase γ through binning phase space in B- → DK-, D → K+π − π − π+ decays*, Physics Letters B **802** (2020) 135188.

[49] S. Harnew *et al.*, *Model-independent determination of the strong phase difference between D0 and D¯0→π+π − π+π − $$ {\overline{D}}\hat{0}\to {\pi}\hat{+}{\pi}\hat{-}{\pi}\hat{+}{\pi}\hat{-} $$amplitudes*, Journal of High Energy Physics **2018** (2018) 144.

[50] R. H. Dalitz, *CXII. On the analysis of τ-meson data and the nature of the τ-meson*, The London, Edinburgh, and Dublin Philosophical Magazine and Journal of Science **44** (1953) 1068.

[51] BaBar Collaboration *et al.*, *Measurement of $\mathrm{cos}2\ensuremath{\beta}$ in ${B}\hat{0}\ensuremath{\rightarrow}{D}\hat{}\mathbf{(}*\m with $D\ensuremath{\rightarrow}{S}\hat{0}{\ensuremath{\pi}}\hat{+}{\ensuremath{\pi}}\hat{\ens }}$ decays by a combined time-dependent Dalitz plot analysis of BaBar and Belle data*, Physical Review D **98** (2018) 112012.

[52] S. U. Chung *et al.*, *Partial wave analysis in K-matrix formalism*, Annalen der Physik **507** (1995) 404.

[53] D. Aston *et al.*, *A study of K-π+ scattering in the reaction K-p→K-π+n at 11 GeV/c*, Nuclear Physics B **296** (1988) 493.

[54] A. Bondar, *Proceedings of BINP special analysis meeting on Dalitz analysis, 24-26 Sep. 2002, unpublished.*

[55] A. Giri, Y. Grossman, A. Soffer, and J. Zupan, *Determining $\ensuremath{\gamma}$ using ${B}^{\pm}\ensuremath{\rightarrow}{\mathrm{DK}}^{\pm}$ with multibody D decays*, Physical Review D **68** (2003) 054018.

[56] BaBar collaboration, B. Aubert *et al.*, *Measurement of the Cabibbo-Kobayashi-Maskawa angle γ in $B^{\mp} \to D^{(*)}K^{\mp}$ decays with a Dalitz analysis of $D \to K^0_S\pi^-\pi^+$*, Phys. Rev. Lett. **95** (2005) 121802, arXiv:hep-ex/0504039.

[57] BaBar collaboration, B. Aubert *et al.*, *Improved measurement of the CKM angle γ in $B^{\mp} \to D^{(*)}K^{(*)\mp}$ decays with a Dalitz plot analysis of D decays to $K^0_S\pi^+\pi^-$ and $K^0_S K^+K^-$*, Phys. Rev. **D78** (2008) 034023, arXiv:0804.2089.

[58] BaBar collaboration, P. del Amo Sanchez *et al.*, *Evidence for direct CP violation in the measurement of the Cabibbo-Kobayashi-Maskawa angle γ with $B^{\mp} \to D^{(*)}K^{(*)\mp}$ decays*, Phys. Rev. Lett. **105** (2010) 121801, arXiv:1005.1096.

[59] Belle collaboration, A. Poluektov *et al.*, *Measurement of ϕ_3 with Dalitz plot analysis of $B^{\pm} \to D^{(*)}K^{\pm}$ decay*, Phys. Rev. **D70** (2004) 072003, arXiv:hep-ex/0406067.

[60] Belle collaboration, A. Poluektov *et al.*, *Measurement of ϕ_3 with Dalitz plot analysis of $B^{+} \to D^{(*)}K^{(*)+}$ decay*, Phys. Rev. **D73** (2006) 112009, arXiv:hep-ex/0604054.

[61] Belle collaboration, A. Poluektov *et al.*, *Evidence for direct CP violation in the decay $B^{\pm} \to D^{(*)}K^{\pm}$, $D \to K^0_S\pi^+\pi^-$ and measurement of the CKM phase ϕ_3*, Phys. Rev. **D81** (2010) 112002, arXiv:1003.3360.

[62] LHCb collaboration, R. Aaij *et al.*, *Measurement of CP violation and constraints on the CKM angle γ in $B^{\pm} \to DK^{\pm}$ with $D \to K^0_S\pi^+\pi^-$ decays*, Nucl. Phys. **B888** (2014) 169, arXiv:1407.6211.

[63] LHCb collaboration, R. Aaij *et al.*, *Measurement of the CKM angle γ using $B^0 \to DK^{*0}$ with $D \to K^0_S\pi^+\pi^-$ decays*, JHEP **08** (2016) 137, arXiv:1605.01082.

[64] A. Bondar and A. Poluektov, *Feasibility study of model-independent approach to Φ3 measurement using Dalitz plot analysis*, The European Physical Journal C - Particles and Fields **47** (2006) 347.

[65] A. Bondar and A. Poluektov, *The use of quantum-correlated D0 decays for Φ3 measurement*, The European Physical Journal C **55** (2008) 51.

[66] Belle collaboration, H. Aihara *et al.*, *First measurement of ϕ_3 with a model-independent Dalitz plot analysis of $B^\pm \to DK^\pm$, $D \to K^0_S\pi^+\pi^-$ decay*, Phys. Rev. **D85** (2012) 112014, arXiv:1204.6561.

[67] LHCb collaboration, R. Aaij *et al.*, *A model-independent Dalitz plot analysis of $B^\pm \to DK^\pm$ with $D \to K^0_S h^+h^-$ ($h = \pi, K$) decays and constraints on the CKM angle γ*, Phys. Lett. **B718** (2012) 43, arXiv:1209.5869.

[68] CLEO Collaboration *et al.*, *Model-independent determination of the strong-phase difference between ${D}\hat{}{0}$ and ${\overline{D}}\hat{}{0}\ensuremath{\rightarrow}{K}_{S,L}\hat{}{0}{h}\hat{}{+}{h}\hat{}\ensuremath{-}$ ($h=\ensuremath{\pi}$, K) and its impact on the measurement of the CKM angle $\ensuremath{\gamma}/{\ensuremath{\phi}}_{3}$*, Physical Review D **82** (2010) 112006.

[69] M. Ablikim *et al.*, *Model-independent determination of the relative strong-phase difference between $D\hat{0}$ and $\bar{D}\hat{0}\rightarrow K\hat{0}_{S,L}\pi\hat{+}\pi\hat{-}$ and its impact on the measurement of the CKM angle γ/ϕ_3*, arXiv:2003.00091 [hep-ex] (2020) arXiv:2003.00091.

[70] R. Aaij *et al.*, *Near-threshold $D\overline{D}{}^0$ spectroscopy and observation of a new charmonium state*, Journal of High Energy Physics **2019** (2019) 35.

[71] C. Thomas and G. Wilkinson, *Model-independent ${D\hat{0}}-{{\overline{D}}\hat{0}}$ mixing and CP violation studies with ${D\hat{0}}\to K_{\mathrm{S}}\hat{0}{\pi\hat{+}}{\pi\hat{-}}$ and ${D\hat{0}}\to K_{\mathrm{S}}\hat{0}{K\hat{+}}{K\hat{-}}$*, Journal of High Energy Physics **2012** (2012) 185.

[72] LHCb collaboration, R. Aaij *et al.*, *Measurement of the CKM angle γ using $B^\pm \to DK^\pm$ with $D \to K^0_S\pi^+\pi^-$, $K^0_S K^+K^-$ decays*, JHEP **10** (2014) 097, arXiv:1408.2748.

[73] Y. Grossman and M. Savastio, *Effects of K-\bar K mixing on determining gamma from B\^pm -> DK\^pm*, Journal of High Energy Physics **2014** (2014) , arXiv:1311.3575.

[74] J. Garra Ticó, *A strategy for a simultaneous measurement of CP violation parameters related to the CKM angle γ in multiple B meson decay channels*, arXiv:1804.05597.